

Proceedings of the Institution of Mechanical Engineers, Part J: Journal of Engineering Tribology

<http://pij.sagepub.com/>

A study of two lobe non recessed worn journal bearing operating with non-Newtonian lubricant

Prashant B Kushare and Satish C Sharma

Proceedings of the Institution of Mechanical Engineers, Part J: Journal of Engineering Tribology 2013 227: 1418 originally published online 8 August 2013

DOI: 10.1177/1350650113496083

The online version of this article can be found at:
<http://pij.sagepub.com/content/227/12/1418>

Published by:



<http://www.sagepublications.com>

On behalf of:



[Institution of Mechanical Engineers](#)

Additional services and information for *Proceedings of the Institution of Mechanical Engineers, Part J: Journal of Engineering Tribology* can be found at:

Email Alerts: <http://pij.sagepub.com/cgi/alerts>

Subscriptions: <http://pij.sagepub.com/subscriptions>

Reprints: <http://www.sagepub.com/journalsReprints.nav>

Permissions: <http://www.sagepub.com/journalsPermissions.nav>

Citations: <http://pij.sagepub.com/content/227/12/1418.refs.html>

>> [Version of Record](#) - Nov 12, 2013

[OnlineFirst Version of Record](#) - Aug 8, 2013

[What is This?](#)

A study of two lobe non recessed worn journal bearing operating with non-Newtonian lubricant

Proc IMechE Part J:
J Engineering Tribology
227(12) 1418–1437
© IMechE 2013
Reprints and permissions:
sagepub.co.uk/journalsPermissions.nav
DOI: 10.1177/1350650113496083
pij.sagepub.com



Prashant B Kushare and Satish C Sharma

Abstract

The present paper is aimed to investigate theoretically the effect of non-linear behavior of the lubricant on the performance of an orifice compensated two lobe non recessed worn hybrid journal bearing. A non-linear behavior of lubricating oil is modeled by using the cubic shear stress law. Dufrane's abrasive model has been used for the analysis of wear damage on the bearing surface. A modified form of Reynolds' equation is solved by using finite element method (FEM) taking into account the relation between shear stress and shear strain rate. The influence of non-linearity factor (\bar{K}) and the wear depth parameter ($\bar{\delta}_w$) on the bearing performance of a two lobe non recessed hybrid journal bearing is presented for the different values of the offset factor ($\bar{\delta} = 0.80, 1.0$ and 1.20). The numerically simulated results indicate that the direct fluid-film stiffness coefficients \bar{S}_{11} and \bar{S}_{22} of worn symmetric bearing configuration ($\bar{\delta} = 1.20$) operated with non-Newtonian lubricant are reduced about 30% and 18%, respectively, vis-à-vis the circular unworn hole entry journal bearing lubricated with Newtonian lubricant. Further, it is also noticed that two lobe non recessed worn hybrid journal bearing with offset factor greater than one results in an enhancement by the order of 11% in the value of \bar{S}_{22} and 6% in the value of $\bar{\omega}_{th}$ as compared to circular worn symmetric hybrid journal bearing operated with non-Newtonian lubricant. The bearing with offset factor less than one is prevalingly suffering by the non-linear behavior of lubricant and wear defect.

Keywords

Non-Newtonian, wear, hybrid journal bearing

Date received: 3 February 2013; accepted: 11 June 2013

Introduction

The non-circular bearings are extensively used in high speed application in industry, as they are simple, efficient and economically viable and provide improved stability. In non-circular journal bearing configurations, the two lobe journal bearing is most commonly used configurations. Its suitability mainly stems from the viewpoint of excellent dynamic performance and better stability over circular bearings. Continuous technological advancement related to high speed modern machineries puts stringent constraints on the design of the bearings. Thus, the bearing needs to be designed on the basis of accurate and realistic design data. In recent years, many researchers have focused their research efforts on non-circular journal bearing configurations. The literature available in the area of non-circular journal bearings is quite exhaustive. Many analytical and experimental studies have been reported in the literature.^{1–13} In the past decades majority of bearing studies have been carried out to evaluate the mode of bearing failure.^{7,11,12,14,15} In continuous operating machinery, the

bearing is expected to be run over a number of cycles and is subjected to frequent rotor rubs during machine start/stop operations. Throughout these transitory periods, the bearing bush gradually gets worn out owing to abrasive action. As a result of this, the bearing geometry is changed. It reveals that unworn analysis of bearing does not give a true performance of the bearing. So, it becomes imperative to consider the influence of wear to predict the performance of two lobe hole entry non recessed hybrid journal bearing realistically. Many experimental and analytical studies related to the effect of wear due to transient start/stop operations in the performance of bearings have been carried out and reported in the literature.^{12,13,15–22,24,36} The first occurrence of wear

Department of Mechanical and Industrial Engineering, Tribology Laboratory, Indian Institute of Technology, Roorkee, India

Corresponding author:

Prashant B Kushare, Department of Mechanical and Industrial Engineering, Tribology Laboratory, Indian Institute of Technology, Roorkee 247667, India.
Email: pbkushare@gmail.com

in the circular hydrostatic journal bearing was reported by Redcliff and Vohr.²³ They reported a wear of about 10% of radial clearance after 10 start/stop operations in the case of cryogenic rocket engine turbo pump bearings. Dufrane et al.²⁴ studied the wear mechanism in fluid-film bearings subjected to frequent start/stop operations. It was reported that the wear damage usually happens symmetrically on all time bottom surface. This worn region was first modeled then experimentally validated by them. Several investigations have also been reported in literature concerning Dufrane's model to study the influence of wear on the bearing performance. The influence of wear on hydrostatic journal bearing was investigated by Soulas and Andres.¹⁶ They compared the numerically simulated results with the available experimental results of Laurant and Childs.¹⁷ Dufrane's model has provided a good approximation with experimental studies of Fillon and Bouyer.²¹ Awasthi et al.,¹⁵ theoretically studied the influence of wear on the performance of the non recessed circular hybrid journal bearing. Phalle et al.¹² and Sharma et al.¹³ presented the theoretical investigation of influence of wear on the performance of non-circular recessed hybrid journal bearing by FEM. They reported that wear significantly affects the bearing performance in case of two lobe recessed hybrid journal bearing.

In order to enhance the lubricating performance of lubricating oil in bearing, increasing use of Newtonian lubricants blended with additives is made. Many lubrication engineers have claimed that the performance of bearing gets improved by using viscosity index improver. The viscosity index (VI) improvers like polymethacrylate or polyisobutylene are high molecular weight polymers which enhance the viscosity of the lubricants. The addition of these additives causes commercial lubricants to behave as non-Newtonian fluids. These lubricants do not obey the Newtonian postulate which assumes a linear relationship between shear stress and rate of shear and the analysis of bearing operating with these lubricant, does not give a factual performance of the bearing. In dynamically loaded bearings, it is important to predict and assess the performance of lubricants over a wide range of dynamic operating conditions hence, to envisage the performance characteristics of a hole entry hybrid journal bearing pragmatically, the effect of non-Newtonian lubricant must be considered in the study.

In recent times, many studies related to the effect of non-Newtonian lubricant on the performance of bearings have been carried out and reported in the literature.^{25–30}

Li et al.²⁵ analyzed the influence of lubricant properties on the dynamics of two-dimensional journal bearings. Prasad²⁶ reported the effects of viscosity and clearance ratios on the performance and design of a hydrodynamic cylindrical bearing and developed

technique give a more realistic approach for the design and performance evaluation of a bearing than conventional methods.

Tayal et al.²⁸ obtained static and dynamic performance characteristics of hydrodynamic journal bearing by using the cubic shear stress law. Zhenming and Don²⁹ studied theoretically and experimentally the non-Newtonian effects of powder lubricant slurries in hydrostatic and squeeze-film bearings. The performance characteristics of the circular hydrostatic journal bearing lubricated with non-Newtonian lubricant was investigated by Sinhasan and Sah.³⁰ The study carried out by Sharma et al.^{31,32} indicates that the combined influence of non-linear behavior of lubricant and bearing flexibility alters the bearing performance characteristics of a slot-entry hybrid journal bearing and orifice compensated hydrostatic journal bearing. They found a decrease in minimum film thickness is of the order of 51.41% relating to the rigid bearing operating with Newtonian lubricant. Nagaraju et al.³³ investigated the combined influence of surface roughness and thermal effects on the performance of a hole-entry hybrid journal bearing system lubricated non-Newtonian behavior of the lubricant.

A thorough scan of the available literature concerning the non-circular hydrostatic/hybrid journal bearings reveals that there exists very limited information related to the behavior of non-circular hole entry hydrostatic/hybrid journal bearings. To the best of the author's knowledge, no study has yet been reported in literature that addresses the combined influence of wear on the performance of two lobe hole entry hybrid journal bearing system operating with non-Newtonian lubricant. Therefore, to bridge the gap in literature, the present study is aimed to numerically evaluate the performance of orifice compensated two lobe non recessed hybrid journal bearing by accounting the influence the non-linear behavior of lubricating oil and wear on the bearing surface.

Two lobe hole entry hybrid journal bearing configuration has been developed to combine the features of non-circular and non recessed hybrid journal bearing systems. The change in the profile of the circular journal bearing has been accounted by defining non-dimensional offset factor (δ). In the present study, symmetric and asymmetric two lobe hole entry worn journal bearing configurations having 12 holes and 6 holes per row, respectively, shown in Figure 1(a) and (b) are considered. The numerically simulated results presented in the paper are expected to be quite useful to the bearing designers and the academic community.

Governing equations

The generalized Reynolds equation governing laminar flow of a variable viscosity lubricant in the

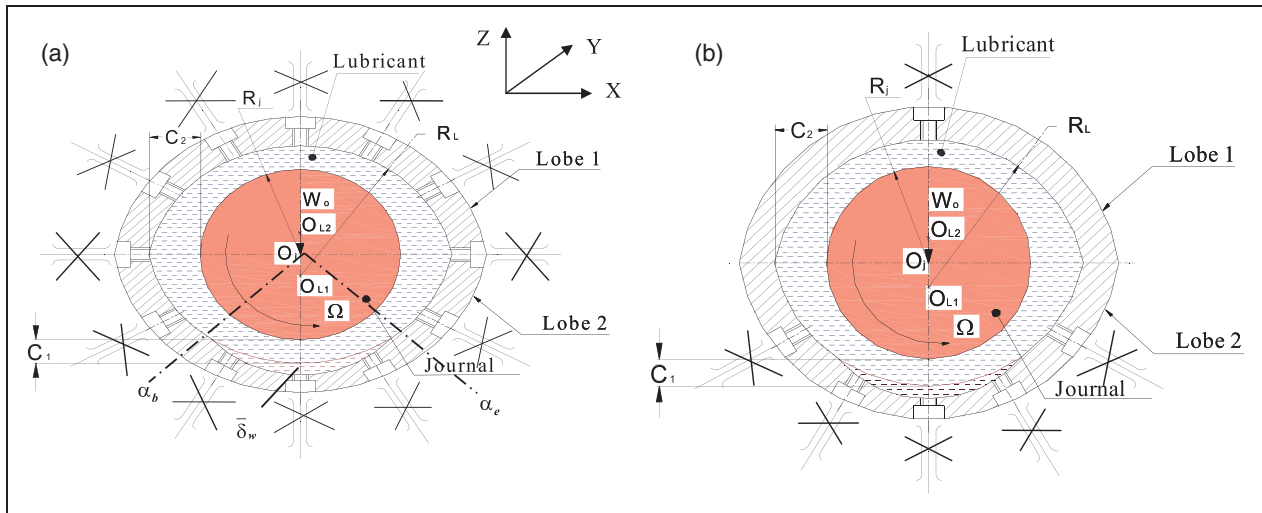


Figure 1. (a) Two lobe symmetric hole entry hybrid journal bearing system. (b) Two lobe asymmetric hole entry hybrid journal bearing system.

clearance space of a journal bearing and the usual assumption is expressed,^{30,31,34} in non-dimensional form as:

$$\frac{\partial}{\partial \alpha} \left(\bar{h}^3 \bar{F}_2 \frac{\partial \bar{p}}{\partial \alpha} \right) + \frac{\partial}{\partial \beta} \left(\bar{h}^3 \bar{F}_2 \frac{\partial \bar{p}}{\partial \beta} \right) = \Omega \left[\frac{\partial}{\partial \alpha} \left\{ \left(1 - \frac{\bar{F}_1}{\bar{F}_0} \right) \bar{h} \right\} \right] + \frac{\partial \bar{h}}{\partial t} \quad (1)$$

where \bar{F}_0 , \bar{F}_1 , and \bar{F}_2 are the cross film viscosity integrals and are given by the following relations:

$$\begin{aligned} \bar{F}_0 &= \int_0^1 \frac{1}{\bar{\mu}} d\bar{z}, \quad \bar{F}_1 = \int_0^1 \frac{\bar{z}}{\bar{\mu}} d\bar{z} \\ \bar{F}_2 &= \int_0^1 \frac{\bar{z}}{\bar{\mu}} \left(\bar{z} - \frac{\bar{F}_1}{\bar{F}_0} \right) d\bar{z} \end{aligned} \quad (2)$$

Minimum fluid-film thickness

The non-dimensional form of fluid-film thickness expression for a multilobe non recessed hybrid journal bearing system can be expressed as^{8,9,12}:

$$\bar{h}_0 = \frac{1}{\delta} - (\bar{X}_j + \bar{x} - \bar{X}_L^i) \cos \alpha - (\bar{Z}_j + \bar{z} - \bar{Z}_L^i) \sin \alpha \quad (3)$$

where \bar{X}_j and \bar{Z}_j are the equilibrium co-ordinates of the journal center, \bar{X}_L^i and \bar{Z}_L^i are the lobe center coordinates of the lobe.

Following the experimentally validated²¹ abrasive wear model of Dufrane et al.,²⁴ worn zone of the bearing is considered. This model assumed that the worn arc at a radius larger than the radius of

the journal. The geometry of the worn out bearing is shown schematically in Figure 1(a). The change in the bush geometry is expressed as^{12,21,22,24}:

$$\begin{aligned} \partial \bar{h} &= \bar{\delta}_w - 1 - \sin \alpha, \quad \text{for } \alpha_b \leq \alpha \leq \alpha_e \\ \partial \bar{h} &= 0; \quad \text{for } \alpha < \alpha_b \text{ or } \alpha > \alpha_e \end{aligned}$$

By accounting the change in bush geometry, the value of fluid-film thickness for two lobe hole entry worn hybrid journal bearing system, is defined as:

$$\bar{h} = \bar{h}_0 + \partial \bar{h} \quad (4)$$

Restrictor flow equation

The equation for the flow of non-Newtonian fluids through orifice restrictor is expressed in non-dimensional form as^{15,30,32}:

$$\bar{Q}_R = \bar{C}_{s2} (1 - \bar{p}_c)^{1/2} \quad (5)$$

Cubic shear stress law model

The flow behavior of most of the non-Newtonian oil is adequately represented by the cubic shear stress law model.^{27,28,30} The constitutive relation of this model is expressed in non-dimensional form as:

$$\bar{\tau} + \bar{K} \bar{\tau}^3 = \bar{\gamma} \quad (6)$$

where \bar{K} is known as a non-linearity factor.

For an incompressible non-Newtonian fluid, the shear strain rate ($\bar{\gamma}$) at a point in fluid film is

expressed as:

$$\dot{\gamma} = \left[\left(\frac{\bar{h}}{\bar{\mu}} \frac{\partial \bar{p}}{\partial \alpha} \left(\bar{z} - \frac{\bar{F}_1}{\bar{F}_0} \right) + \frac{\Omega}{\bar{\mu} \bar{h} \bar{F}_0} \right)^2 + \left(\frac{\bar{h}}{\bar{\mu}} \frac{\partial \bar{p}}{\partial \beta} \left(\bar{z} - \frac{\bar{F}_1}{\bar{F}_0} \right) \right)^2 \right]^{1/2} \quad (7)$$

The viscosity of a non-Newtonian lubricant is described by apparent viscosity ($\bar{\mu}_a$) which is defined as a function of shear strain rate ($\dot{\gamma}$)

$$\bar{\mu}_a = \bar{\tau} / \dot{\gamma} \quad (8)$$

Finite element formulation

The lubricant flow field is discretized by using four-noded isoparametric elements. The pressure at a point in the element is assumed to vary linearly and expressed approximately as:

$$\bar{p} = \sum_{j=1}^{n_l^e} \bar{p}_j N_j \quad (9)$$

where N_j is elemental shape function and n_l^e is the number of nodes per element of two-dimensional flow-field discretized solution domain. Using Galerkin's orthogonality conditions and following the usual assembly procedure, the global system equation is obtained as^{12,30,32}:

$$[\bar{F}] \{\bar{P}\} = \{\bar{Q}\} + \Omega \{\bar{R}_H\} + \bar{X}_J \{\bar{R}_x\} + \bar{Z}_J \{\bar{R}_z\} \quad (10)$$

where

$[\bar{F}]$ = assembled fluidity matrix,
 $\{\bar{p}\}$ = nodal pressure vector,
 $\{\bar{Q}\}$ = nodal flow vector,
 $\{\bar{R}_H\}$ = column vectors due to hydrodynamic terms and
 $\{\bar{R}_x\}, \{\bar{R}_z\}$ = global right hand side vector due to journal center velocities.

For e th element these are given by:

$$\bar{F}_{ij}^e = \int_{\Omega^e} \bar{h}^3 \left[\bar{F}_2 \frac{\partial N_i}{\partial \alpha} \frac{\partial N_j}{\partial \alpha} + \bar{F}_2 \frac{\partial N_i}{\partial \beta} \frac{\partial N_j}{\partial \beta} \right] d\Omega^e \quad (10a)$$

$$\bar{Q}_i^e = \int_{\Gamma^e} \left\{ \left(\bar{h}^3 \bar{F}_2 \frac{\partial \bar{p}}{\partial \alpha} - \Omega \left(1 - \frac{\bar{F}_1}{\bar{F}_0} \right) \bar{h} \right) l_1 + \left(\bar{h}^3 \bar{F}_2 \frac{\partial \bar{p}}{\partial \beta} \right) l_2 \right\} N_i d\Gamma^e \quad (10b)$$

$$\bar{R}_{H_i}^e = \int_{\Omega^e} \left(1 - \frac{\bar{F}_1}{\bar{F}_0} \right) \bar{h} \frac{\partial N_i}{\partial \alpha} d\Omega^e \quad (10c)$$

$$\bar{R}_{x_i}^e = \int_{\Omega^e} N_i \cos \alpha d\Omega^e \quad (10d)$$

$$\bar{R}_{z_i}^e = \int_{\Omega^e} N_i \sin \alpha d\Omega^e \quad (10e)$$

where l_1 and l_2 are direction cosines and $i, j = 1, 2, \dots, n_l^e$ (number of nodes per element).

Ω^e refers to the area domain and Γ^e is the boundary of the e th element. The element matrices are generated for all elements and are assembled to obtain a global matrix.

Boundary conditions

The boundary conditions used in the lubricant flow field are described as^{22,32}:

- (a) Nodes situated on the external boundary of the bearing have zero relative pressure with respect to ambient temperature;

$$\bar{p}|_{\beta=\mp 1.0} = 0.0 \quad (11a)$$

- (b) Nodes situated on holes have equal pressure.
 (c) Flow of lubricant through the restrictor is equal to the bearing input flow.
 (d) At the trailing edge of the positive region.

$$\bar{p} = \frac{\partial \bar{p}}{\partial \alpha} = 0.0 \quad (11b)$$

Solution procedure

Study lobed hole entry worn hybrid journal bearing system operating with non-Newtonian lubricant needs an iterative scheme to establish the solution of lubricant flow field system equation (10) with orifice flow restrictor equation (5) and apparent viscosity ($\bar{\mu}_a$) equation (8) as a constraint along with appropriate boundary condition. To find the FEM solution, the lubricant flow field in the clearance space of a bearing is discretized with rectangular mesh of 36×4 division, equally spaced in X and Y directions, respectively. This grid has total number of 144 quadrilateral isoparametric elements consisting of 168 nodes. The flow chart of an iterative scheme used to obtain the converged solution has been shown in Figure 2. Unit PDATA reads the input data with two dimensional lubrication mesh. Then, assuming steady state condition unit, FLEM computes the values of fluid-film thickness at each nodal point as given by equation (4) utilizing the tentative values of \bar{X}_j, \bar{Z}_j .

The solution for the Newtonian lubricant is obtained as the initial trial solution to be used for the non-Newtonian case. The values of the function \bar{F}_0, \bar{F}_1 and \bar{F}_2 are obtained at each Gauss point using

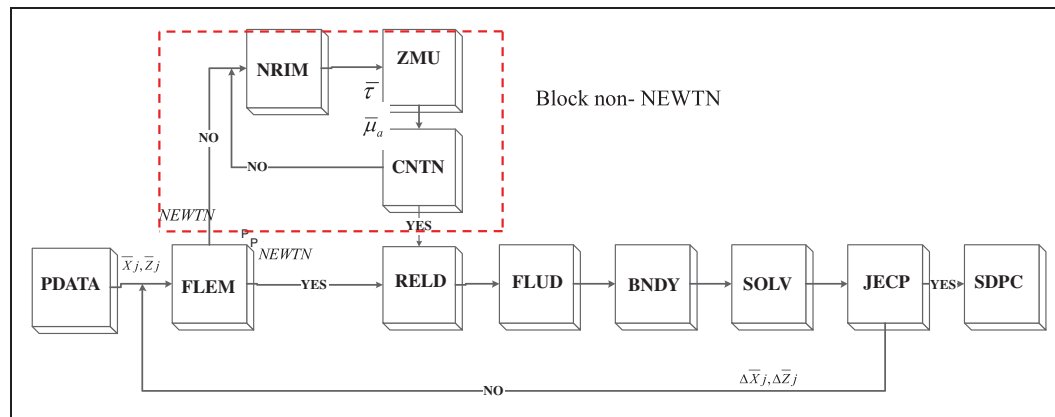


Figure 2. Overall iterative solution scheme.

Table 1. Geometric and operating parameters of two lobe hole-entry hybrid journal bearing.^{12,13,24,35,15,22,27,30,31}

Operating dimensional parameters			Operating non-dimensional parameters			Geometric parameters	
Radius of the journal	R_j	50 mm	Aspect ratio	λ	1.00	No. of holes per row (k)	12
Bearing liner thickness	t_h	5 mm	Land width ratio	a_b/L	0.25		
Bearing length	L	100 mm	External load	\bar{W}_0	1.00	Symmetric bearing configuration	
Radial clearance	c	0.05020 mm	Speed parameter	Ω	1.00		
Shaft speed	N	2500 r/min	Restrictor design parameter	\bar{C}_{s_2}	0.02–0.1	No. of holes per row (k)	6
Supply pressure	p_s	8.96 MN/m ²	Non-linearity factor	\bar{K}	0.0, 1.00	Asymmetric bearing configuration	
External load	W	22.4 kN	Wear Depth parameter	$\bar{\delta}_w$	0.0, 0.5	No. of rows (n)	2
Compensating element	Orifice		Offset factor	δ	0.80, 1.00, 1.20		

numerical integration (Simpson's rule). The shear strain rate ($\dot{\gamma}$) is computed using equation (7) and the corresponding equivalent shear stress ($\bar{\tau}$) is obtained from equation (6) using Newton–Raphson method in NRIM unit. The apparent viscosity ($\bar{\mu}_a$) is computed at each Gauss point using equation (8). The iterative procedure is terminated in unit CNTN when the differences in nodal pressures at each node in the successive iterations become less than the pre-defined tolerance of $ZO \leq 0.001$ for non-Newtonian solution. For the continuity of the flow between restrictor and bearing, the system equation is modified accordingly. Elements of fluidity matrices of equation (10) are generated and assembled in unit FLUD. The unit BNDY modifies the system equation for specified boundary conditions. The modified system equation is solved for the nodal pressure in unit SOLV using the Gauss elimination technique. The equilibrium journal center position corresponding to a specified value of external load is attained in unit JECPC. In the JECPC unit, the specified external load and the load carrying capacity are obtained and are compared in order to

compute journal center increments ($\Delta \bar{X}_j$ and $\Delta \bar{Z}_j$). The iterative process is continued until the difference in journal center coordinates in successive iterations falls below the required tolerance. When the journal center equilibrium position is achieved, unit SDPC computes the static and dynamic performance characteristics of the hybrid journal bearing system.

Results and discussion

The solution scheme as described in the preceding section has been used to compute the performance characteristics of orifice compensated two lobe non recessed worn hybrid journal bearing system operating with non-Newtonian lubricant. The chosen values of the bearing geometric and operating parameters are the most generally used values as shown in Table 1. As mentioned earlier, no results are available in the literature considering symmetric and asymmetric journal bearing configuration for the case of a two lobe non recessed worn hybrid journal bearing lubricated with non-Newtonian lubricant. Therefore, in order to

validate the developed numeric model and adopted solution methodology, the results have been validated with the already reported results of Hashimoto et al.,¹⁸ Wada and Hayashi²⁷ and Lund and Thomsen² for the case of wear study, non-Newtonian lubricants and the two lobe hydrodynamic journal bearing, respectively. For the wear study, the computed results have been compared with the published results of Hashimoto et al.¹⁸ as shown in Figure 3. The numerically simulated results for worn and unworn hydrodynamic plain journal bearing agree quite well with the revealed results with a small deviation of 2–4%. Further, the results of the plain hydrodynamic journal bearing lubricated with non-Newtonian lubricants (cubic shear law) have been computed for a Sommerfeld number to a wide eccentricity ratio for the non-linearity factor $\bar{K} = 0.0$ and $\bar{K} = 0.1$.

The computed results have been also compared with the available results of Wada and Hayashi,²⁷ as shown in Figure 4. The computed value appears to be in good agreement with the published work. The deviation in the results can be attributed due to the

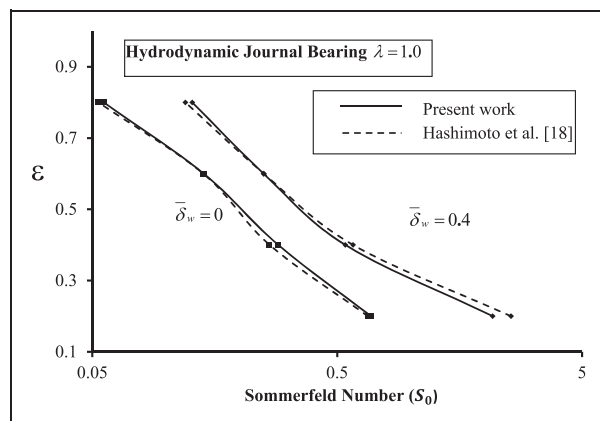


Figure 3. Variation of eccentricity ratio (ε) with Sommerfeld number (S_0).

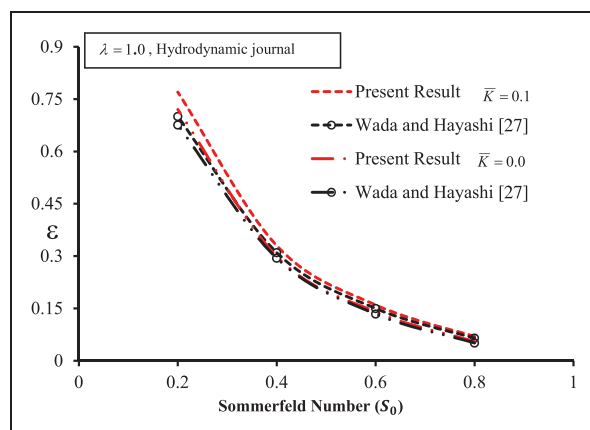


Figure 4. Variation of eccentricity ratio (ε) with Sommerfeld number (S_0).

different computational schemes used in the studies. Further, the performance characteristics of the two lobe hydrodynamic journal bearing have been computed by using developed program and compared with data of Lund and Thomsen.² The results compare very well as shown in Table 2.

Based on the available literature,^{12,13,15,22,24} the maximum value of wear depth parameter $\bar{\delta}_w = 0.5$ has noteworthy result, have been used in the present study, the results have been presented for non-linearity factor $\bar{K} = 0.0, 1.0$ based on literature.^{27,30,31}

The static and dynamic bearing performance characteristics viz. maximum pressure (\bar{P}_{\max}), minimum fluid-film thickness (\bar{h}_{\min}), bearing flow (\bar{Q}), stiffness coefficient ($\bar{S}_{11}, \bar{S}_{22}$), damping coefficient ($\bar{C}_{11}, \bar{C}_{22}$) and threshold speed margin ($\bar{\omega}_{th}$) have been computed and presented for different values of offset factor (δ), restrictor design parameter (\bar{C}_{S_2}), wear depth parameter ($\bar{\delta}_w$) and non-linearity factor (\bar{K}) for non-Newtonian lubricant. $\bar{K} = 0$ represents Newtonian lubricant and $\bar{K} = 1.0$ represent the non-Newtonian behavior of the lubricant. The numerical results have been presented for symmetric and asymmetric journal bearing configuration as a function of restrictor design parameter (\bar{C}_{S_2}) in graphical form as shown in Figures 5 to 21.

Maximum fluid-film pressure (\bar{P}_{\max})

The variation in maximum fluid-film pressure (\bar{P}_{\max}) for different values of offset factor has been presented as the function of restrictor design parameter for symmetric and asymmetric hole entry worn circular and non-circular hybrid journal bearing system as shown in Figures 5 and 6. It is observed that non-circular journal bearing with an offset factor 1.20, $\bar{\delta}_w = 0.5$ and $\bar{K} = 0$ have a larger value of maximum fluid-film pressure (\bar{P}_{\max}) than the non-circular journal bearing with an offset factor 1.20, $\bar{\delta}_w = 0.0$ and $\bar{K} = 0$. This is due to a change in the fluid-film profile.

Table 2. Comparison of bearing performance characteristics of two lobe hydrodynamic journal bearing.

$L/D = 1, \Omega = 1, \delta = 0.5, \bar{W}_o = 5.0$

Bearing characteristics parameters	Present work	Lund and Thomsen ²
ε	0.3426	0.340
ϕ	80.997	82.100
\bar{S}_{xx}/\bar{W}_o	1.203	1.110
\bar{S}_{xz}/\bar{W}_o	1.812	1.700
\bar{S}_{zx}/\bar{W}_o	-3.5004	-3.610
\bar{S}_{zz}/\bar{W}_o	5.1544	5.130
\bar{C}_{xx}/\bar{W}_o	2.801	2.620
$-(\bar{C}_{xz} = \bar{C}_{zx})/\bar{W}_o$	0.2568	0.238
\bar{C}_{zz}/\bar{W}_o	9.3348	9.430

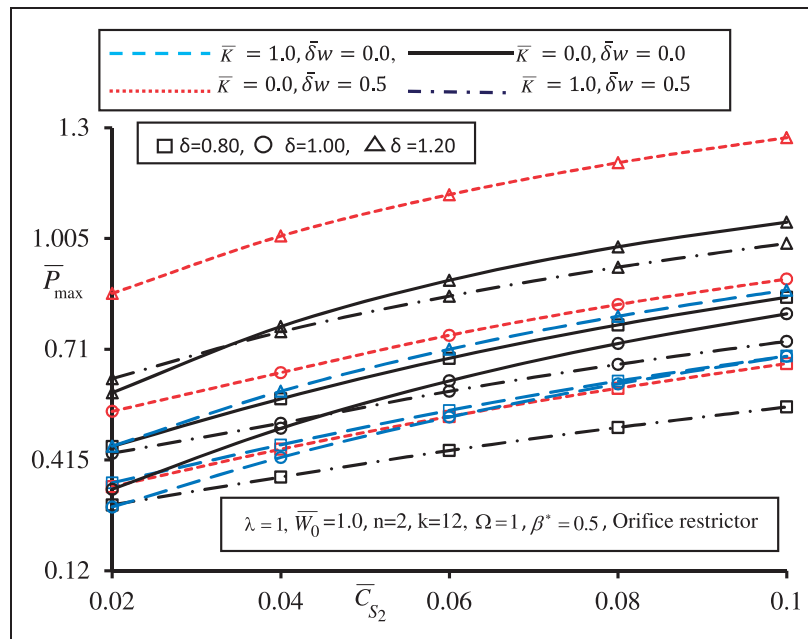


Figure 5. Maximum pressure (\bar{P}_{\max}) for symmetric bearing configuration.

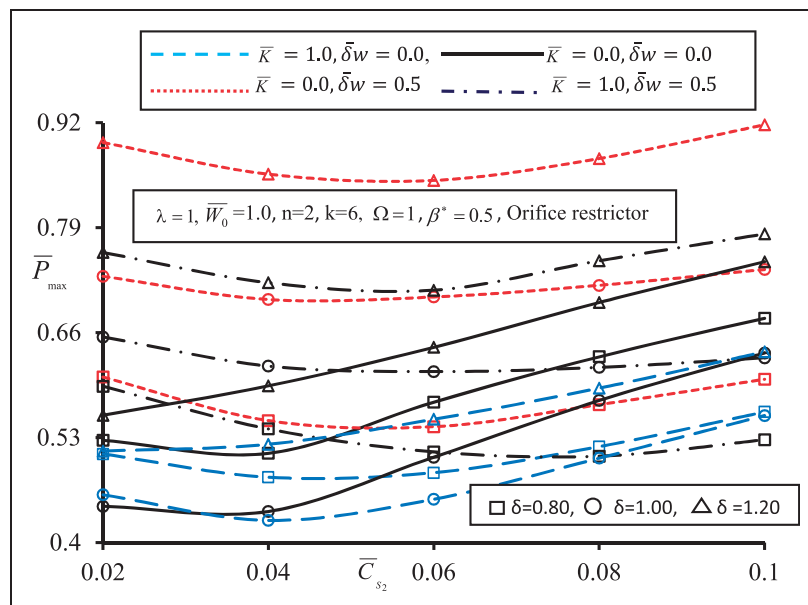


Figure 6. Maximum Pressure (\bar{P}_{\max}) for asymmetric bearing configuration.

The journal tends to move into the worn out region thereby reducing the clearance. This reduced clearance increases the fluid-film pressure to support the applied load. The trends are clearly visible through the three dimensional surface plots of mid-plane surface pressure distribution as shown in Figures 7(a–d). For a chosen value of $\bar{W}_0 = 1.0$ and wear depth ($\bar{\delta}_w$), the value of (\bar{P}_{\max}) for an asymmetric configuration is less than that of a symmetric configuration. A journal bearing with an asymmetric configuration operates at comparatively low eccentricities; therefore, the thickness of the fluid-film profile is comparatively large,

indicating a low value of (\bar{P}_{\max}). For non-Newtonian lubricant, reduction in the values of fluid-film pressure is observed for symmetric and an asymmetric non recessed worn hybrid journal bearing. The fluid-film pressure distribution gets changed due to the non-linear behavior of the lubricants. The fluid-film pressure (\bar{P}_{\max}) gets decreased up to 28% at $\bar{\delta}_w = 0.5$, $\bar{K} = 1$ and $\delta = 1.20$ with respect to the worn journal bearing operating with Newtonian lubricant. Furthermore, it may be observed that non-circular hole entry hybrid journal bearing at $\delta = 1.20$ operating with Newtonian lubricants attains a larger value of

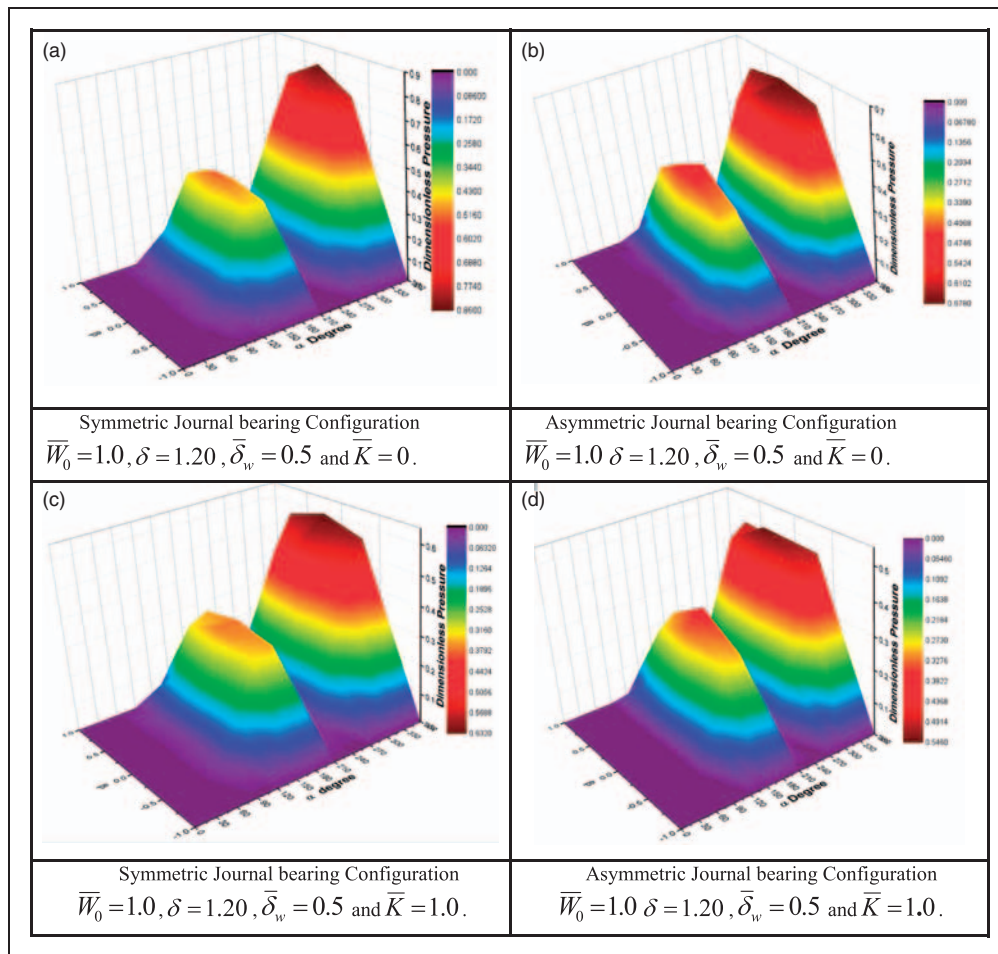


Figure 7. (a–d) Maximum fluid-film pressure (\bar{P}_{\max}). (a) Symmetric journal bearing configuration. $\bar{W}_0 = 1.0, \delta = 1.20, \bar{\delta}_w = 0.5$ and $\bar{K} = 0$. (b) Asymmetric journal bearing configuration. $\bar{W}_0 = 1.0, \delta = 1.20, \bar{\delta}_w = 0.5$ and $\bar{K} = 0$. (c) Symmetric journal bearing configuration. $\bar{W}_0 = 1.0, \delta = 1.20, \bar{\delta}_w = 0.5$ and $\bar{K} = 1.0$. (d) Asymmetric journal bearing configuration. $\bar{W}_0 = 1.0, \delta = 1.20, \bar{\delta}_w = 0.5$ and $\bar{K} = 1.0$.

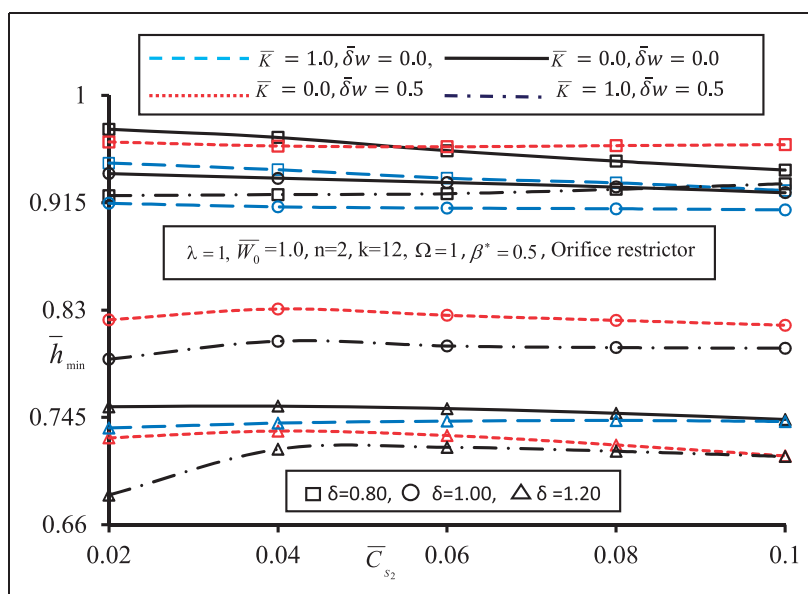


Figure 8. Minimum fluid-film thickness (\bar{h}_{\min}) for symmetric bearing configuration.

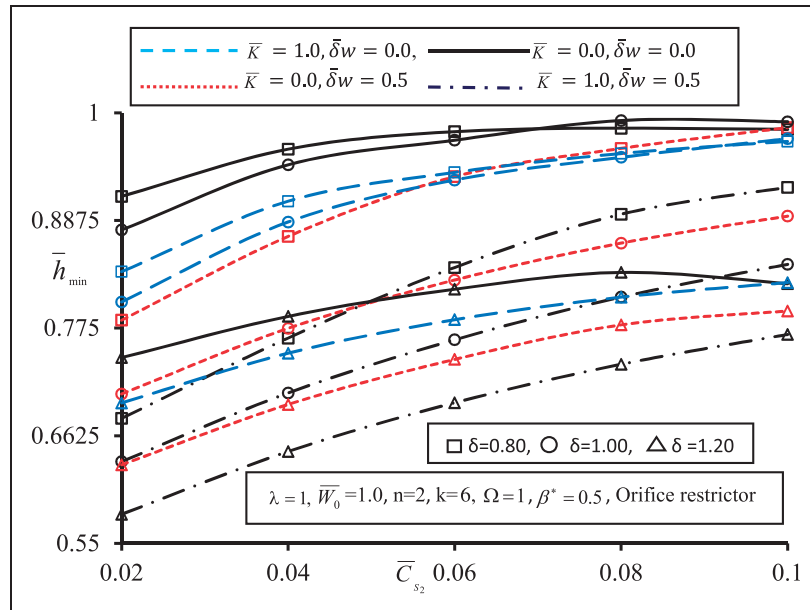


Figure 9. Minimum fluid-film thickness (\bar{h}_{\min}) for asymmetric bearing on configuration.

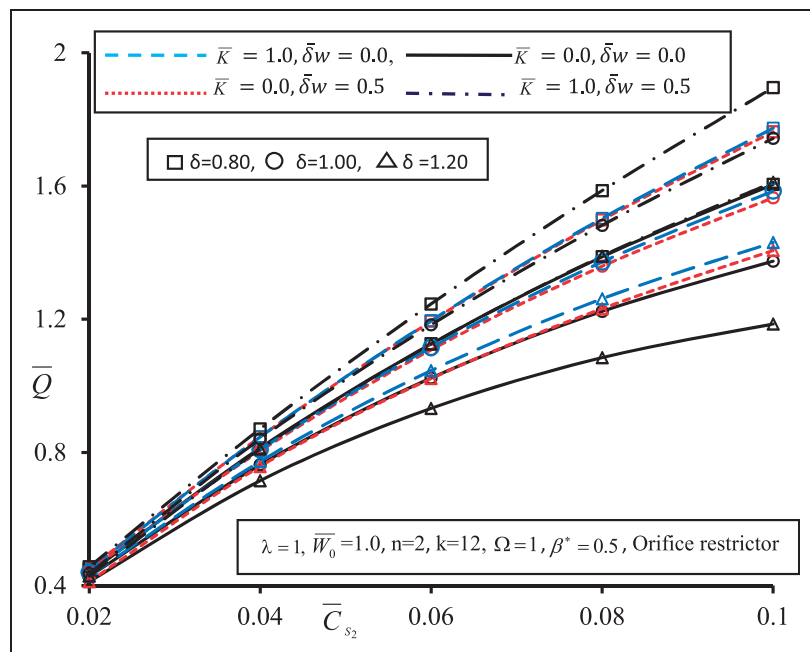


Figure 10. Lubricant flow (\bar{Q}) for symmetric bearing configuration.

maximum fluid-film pressure (\bar{P}_{\max}) than the hole entry circular hybrid journal bearing on the fixed value wear depth parameter ($\delta_w = 0.5$) for a symmetric and an asymmetric bearing configuration.

Minimum fluid-film thickness (\bar{h}_{\min})

Figures 8 and 9 depict the variation in minimum fluid-film thickness (\bar{h}_{\min}) for two lobe non recessed worn hybrid journal bearing system. It is observed that the minimum fluid-film thickness (\bar{h}_{\min}) decreases with an

increase in the non-linearity factor of the lubricant (\bar{K}) for both symmetric and asymmetric bearing configurations. For two lobe hole entry symmetric bearing configuration with offset factor $\delta = 0.80$ and wear depth parameter $\delta_w = 0.5$ provides a larger value of minimum fluid-film thickness (\bar{h}_{\min}) than for the bearing configuration with offset factor $\delta = 1.20$ and 1.00 . This is because of the maximum clearance occurring at the bottom of the bearing with an offset factor of $\delta = 0.80$. As a result of this, more lubricant gets pumped into the clearance space thereby increasing

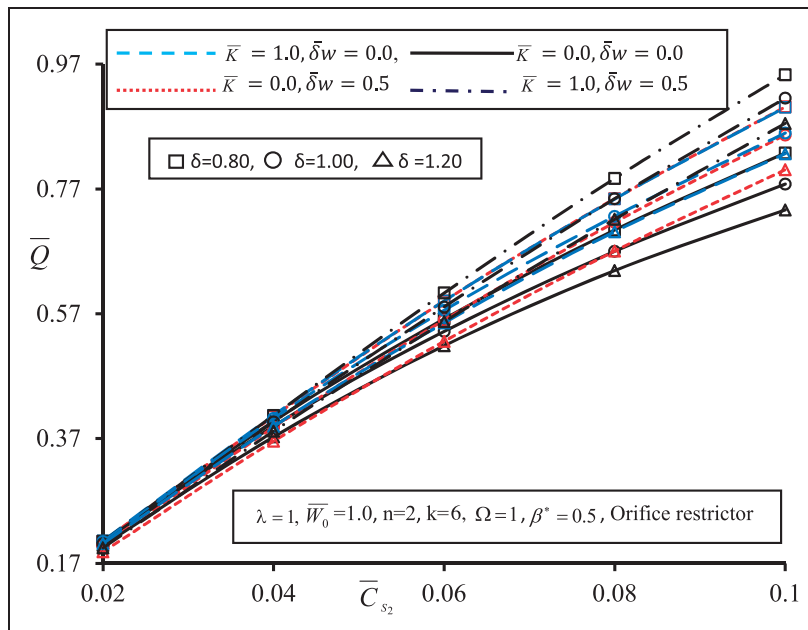


Figure 11. Lubricant flow (\bar{Q}) for asymmetric bearing configuration.

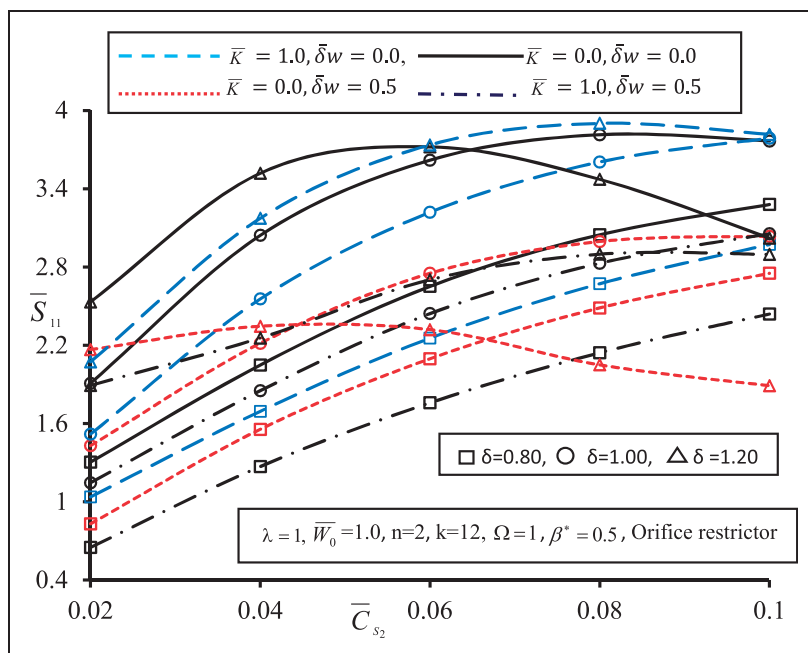


Figure 12. Direct fluid-film stiffness coefficient (\bar{S}_{11}) for symmetric bearing configuration.

the film thickness in the gap. Further, the value of minimum fluid-film thickness (\bar{h}_{\min}) at constant external load is observed to decreased with an increase in the non-linear behavior of lubricant (\bar{K}) for non recessed two lobe hole entry worn hybrid journal bearing. This is because of shear thinning of the lubricant, an effect where a fluid's viscosity decreases with an increasing rate deformation. As a consequence of this, fluid film becomes thinner and journal runs at

lower values of \bar{h}_{\min} compared to journal bearing operating with Newtonian lubricants.

It may also be noticed from Figure 9 that the values of minimum fluid-film thickness (\bar{h}_{\min}) decreases with an increase in the value of the restrictor design parameter for the two lobe non recessed hybrid journal bearing with wear depth parameter ($\bar{\delta}_w = 0.5$). The greater the value of wear depth ($\bar{\delta}_w$), the greater the eccentricity of the bearing and journal tend to go

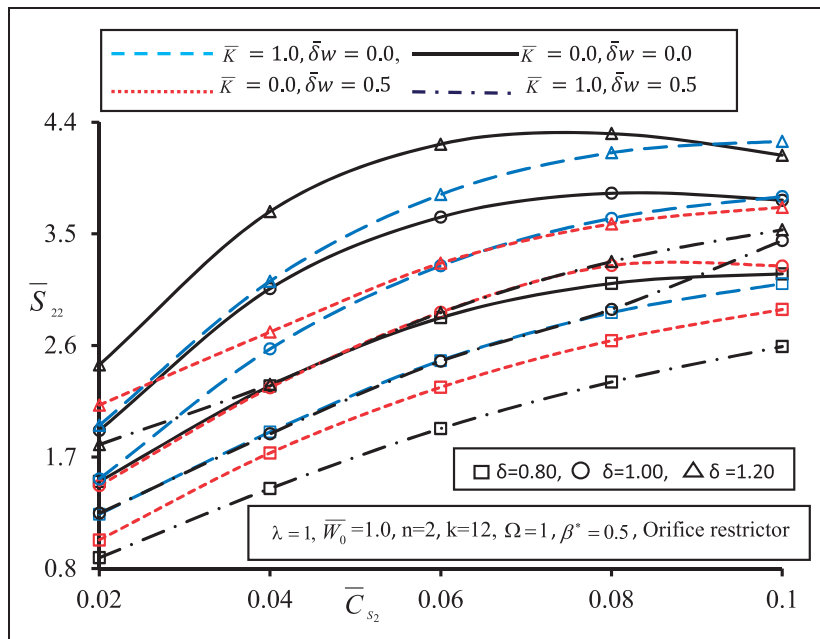


Figure 13. Direct fluid-film stiffness coefficient (\bar{S}_{22}) for symmetric bearing configuration.

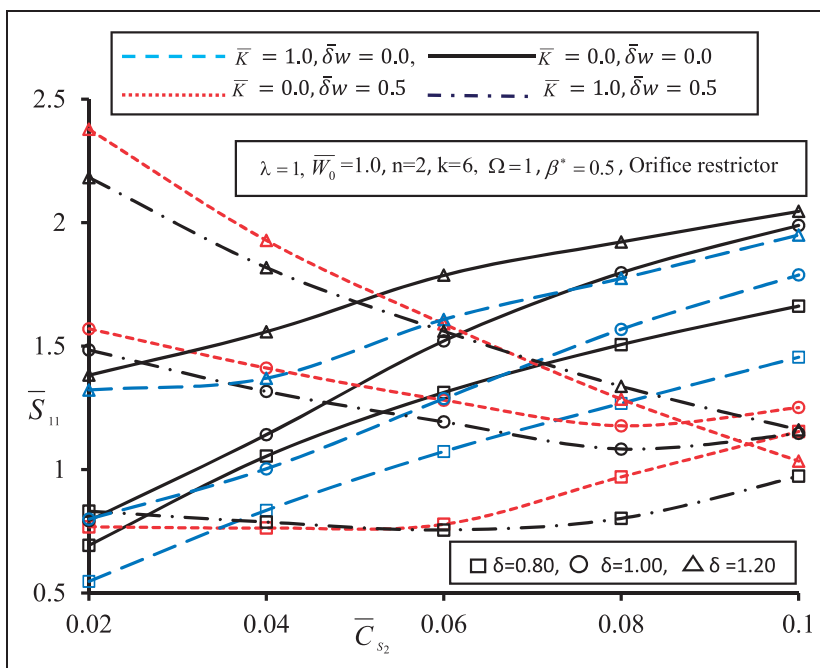


Figure 14. Direct fluid-film stiffness coefficient (\bar{S}_{11}) for asymmetric bearing configuration.

into defect footprint, so the fluid-film thickness reduces for worn bearing. The combined effect of wear depth parameter ($\bar{\delta}_w$) and non-linearity factor (\bar{K}) further lowers the value of (\bar{h}_{\min}) in case of a symmetric bearing configuration. For an asymmetric bearing configuration, the values of minimum fluid-film thickness (\bar{h}_{\min}) decreases with an increase in the value of restrictor design parameter ($\bar{C}_{s2} = 0.06$) for $\bar{\delta}_w = 0.0$ and $\bar{K} = 0$ and $\bar{\delta}_w = 0.0$ and $\bar{K} = 1$. For a

given operating condition of $\bar{\delta}_w = 0.5$, $\bar{K} = 1$ and $\delta = 1.20$, the maximum decrease in fluid-film thickness (\bar{h}_{\min}) is observed to the order of 23.48% and 28.25% for symmetric and asymmetric bearing configuration respectively, when compared with the circular unworn journal bearing operating with Newtonian lubricants. Hence the bearing designer requires a careful selection of values of parameter ($\bar{\delta}_w$) and (\bar{K}) in order to maintain safe operating limit of (\bar{h}_{\min}).

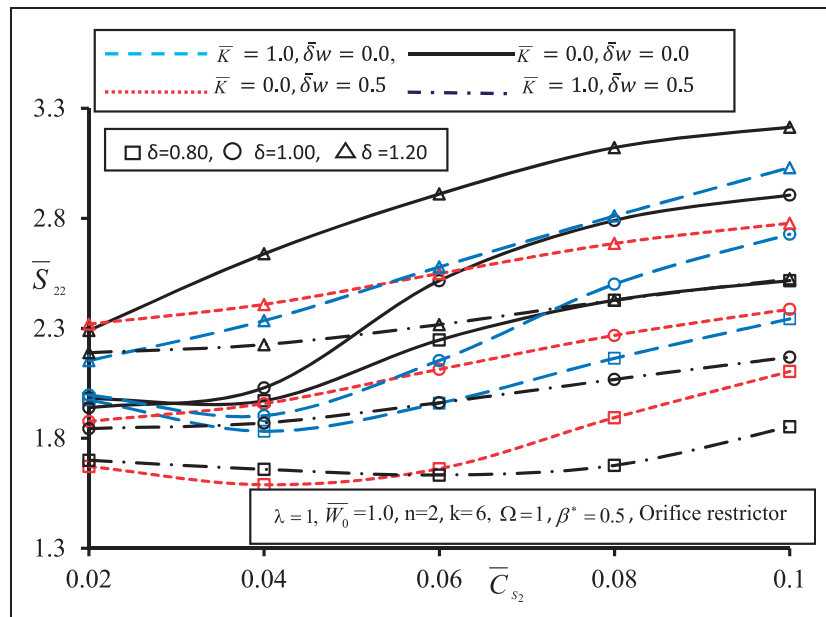


Figure 15. Direct fluid-film stiffness coefficient (\bar{S}_{22}) for asymmetric bearing configuration.

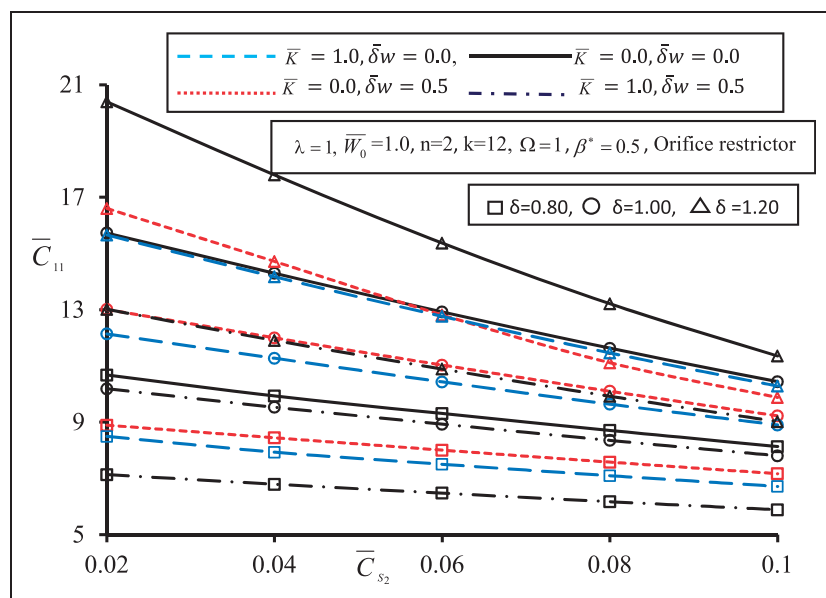


Figure 16. Direct fluid-film damping coefficient (\bar{C}_{11}) for symmetric bearing configuration.

Bearing flow (\bar{Q})

Figures 10 and 11 depict the variation in bearing flow (\bar{Q}) for both the non-circular configurations. It may be seen from Figures 10 and 11, with an increase in the non-linearity factor (\bar{K}), the lubricant becomes more non-linear and results in an increase in the bearing flow (\bar{Q}) for both the bearing configurations. For a symmetric bearing configuration as shown in Figure 10, it is observed that the offset factor $\delta=0.80$ and $\delta_w=0.5$, $\bar{K}=1$ have the largest value of bearing flow (\bar{Q}) than that of the non-circular unworn hybrid journal bearing having an offset factor $\delta=1.20$ for bearing

lubricated with Newtonian lubricant at $\delta_w=0.0$. The increase of a non-linearity factor (\bar{K}), which attributes to the apparent lubricant viscosity variation results into decrease in the bearing load capacity. Therefore, to support the external load (\bar{W}_0), the bearing needs to be pumped with more lubricant thereby increasing the fluid flow (\bar{Q}). Thus, in the bearings operated with non-Newtonian lubricants the pumping power gets increased due to the increase in the fluid flow.

Further, it may be observed that bearing with an offset factor ($\delta=0.80$) and ($\delta=1.0$) have a larger value of bearing flow (\bar{Q}) than the bearing with an

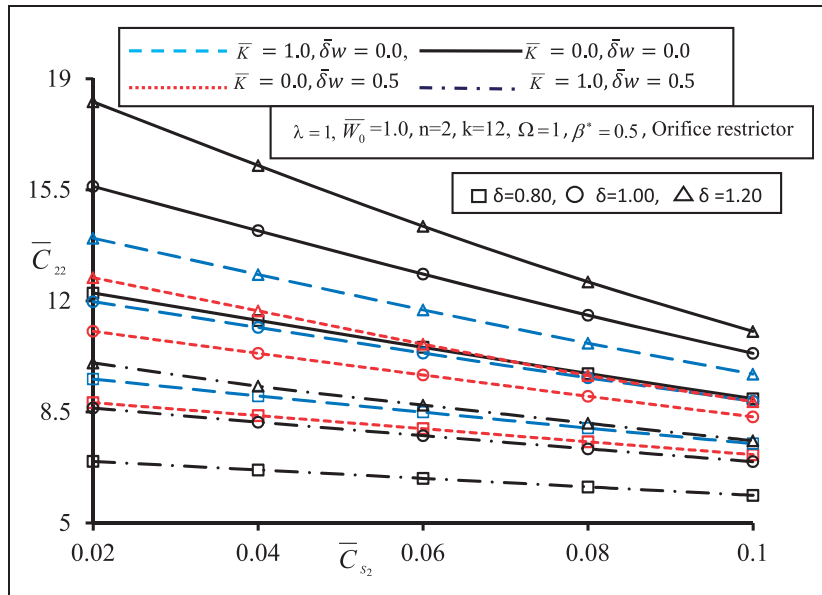


Figure 17. Direct fluid-film damping coefficient (\bar{C}_{22}) for symmetric bearing configuration.

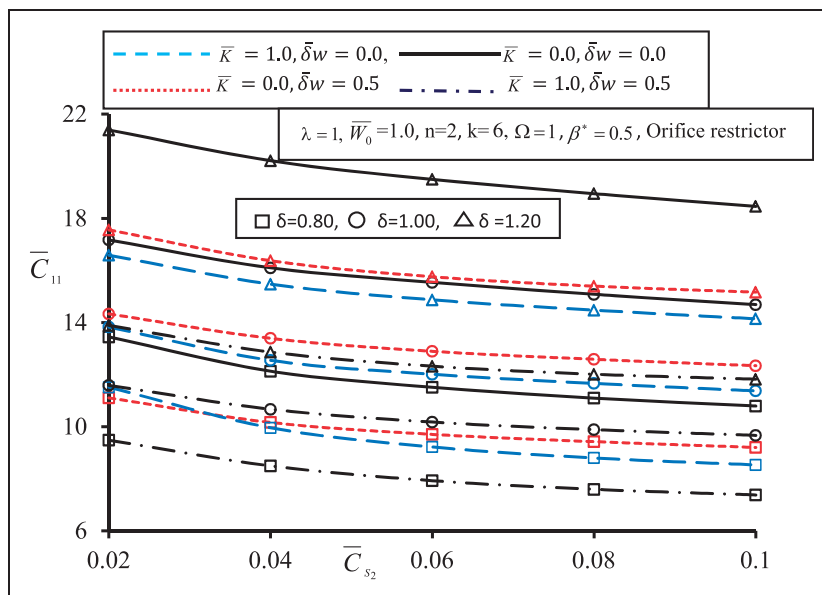


Figure 18. Direct fluid-film damping coefficient (\bar{C}_{11}) for asymmetric bearing configuration.

offset factor ($\delta = 1.20$) at the fixed value of ($\bar{\delta}_w = 0.5$). The offset factor greatly influences the bearing lubricant flow in both the configurations. The bearing with an offset factor ($\delta = 1.20$) operates at the lesser value of bearing flow (\bar{Q}). The trend in the variation of lubricant fluid flow rate is similar to the experimental observation of Laurant and Childs,¹⁷ i.e. an increase of flow rate for worn journal bearing than unworn for circular journal bearing due to larger flow in worn zone. Thus, for the worn out bearing lubricated with non-Newtonian lubricant, the bearing flow gets increased by 10.77% for symmetric bearing configuration. It may be seen that bearing flow (\bar{Q}) is more for a symmetric configuration than for an asymmetric

configuration because of a number of holes. As a consequence of this, a higher flow rate is anticipated from this configuration.

Direct fluid-film stiffness coefficients ($\bar{S}_{11}, \bar{S}_{22}$)

The variation in the value of direct fluid-film stiffness coefficient ($\bar{S}_{11}, \bar{S}_{22}$) has been shown in Figures 12 to 15. From these figures, it is visible that the value of direct fluid-film stiffness coefficient ($\bar{S}_{11}, \bar{S}_{22}$) decreases with the increase in the value of wear depth parameter ($\bar{\delta}_w$). Further, it is noticed that the effect of wear ($\bar{\delta}_w$) is significantly higher on the direct fluid-film stiffness coefficient ($\bar{S}_{11}, \bar{S}_{22}$) for the value of

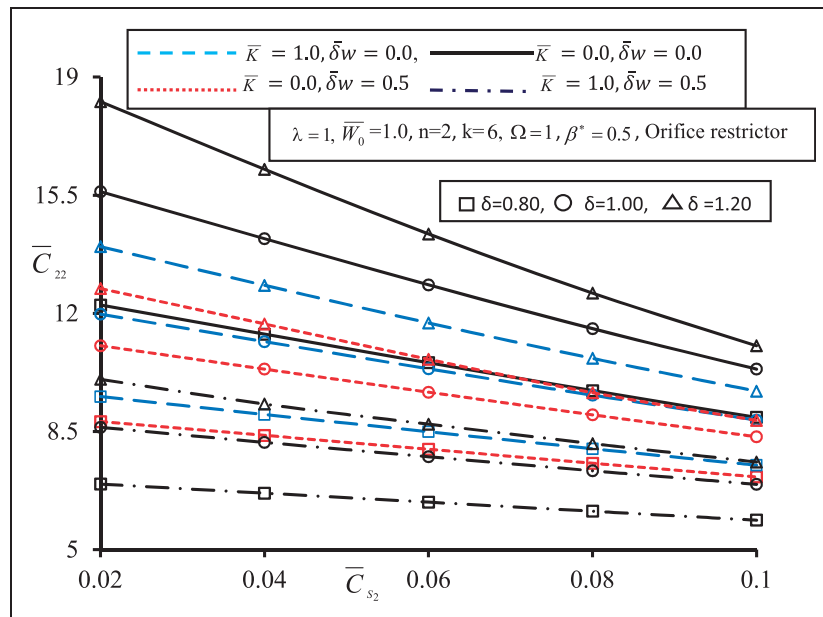


Figure 19. Direct fluid-film damping coefficient (\bar{C}_{22}) for asymmetric bearing configuration.

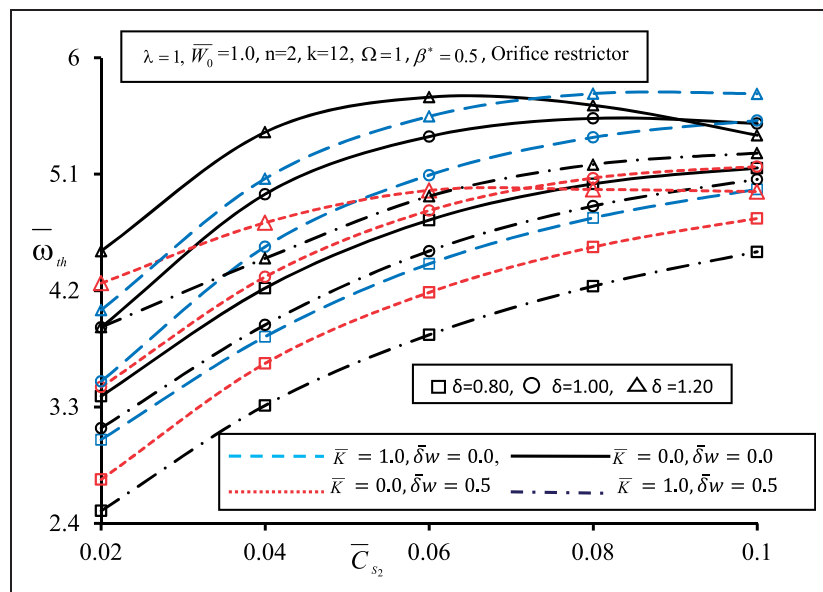


Figure 20. Threshold speed ($\bar{\omega}_{th}$) for symmetric bearing configuration.

restrictor design parameter $\bar{C}_{S_2} > 0.06$. It is also noticed that non-circular hybrid journal bearing with an offset factor of ($\delta = 1.20$) have the largest value of \bar{S}_{11} and \bar{S}_{22} as compared to circular hybrid journal bearing ($\delta = 1.0$) at the fixed value of wear depth of $\bar{\delta}_w = 0.5$. Further, it is also noticed that for a constant value of $\bar{C}_{S_2} > 0.06$, the value of \bar{S}_{11} increases as the lubricant behavior becomes more non-linear. The value of the $\bar{S}_{11}/\bar{S}_{22}$ is minimum for the non-Newtonian lubricants at $\bar{\delta}_w = 0.5$. From Figures 12 to 15, it may be observed that the effect of non-Newtonian behavior of lubricants is to reduce the value of $\bar{S}_{11}/\bar{S}_{22}$ by 6–10% for a chosen value of

$\bar{W}_0 = 1.0, \bar{C}_{S_2} = 0.06$ for a symmetric and an asymmetric bearing configuration.

The combined influence of wear depth ($\bar{\delta}_w = 0.5$) and non-linear behavior of the lubricant ($\bar{K} = 1.0$) is to reduce the value of \bar{S}_{11} and \bar{S}_{22} for both the configuration. The maximum reduction of the order of around 31% and 18% in the values of \bar{S}_{11} and \bar{S}_{22} is found for symmetric bearing configuration at $\delta = 1.20$ and $\bar{C}_{S_2} = 0.06$. Further, it is noticed that the value of stiffness coefficient ($\bar{S}_{11}, \bar{S}_{22}$) is largest for two lobe hole entry a symmetric bearing configuration than the two lobe hole entry an asymmetric bearing configuration for same geometric and operating

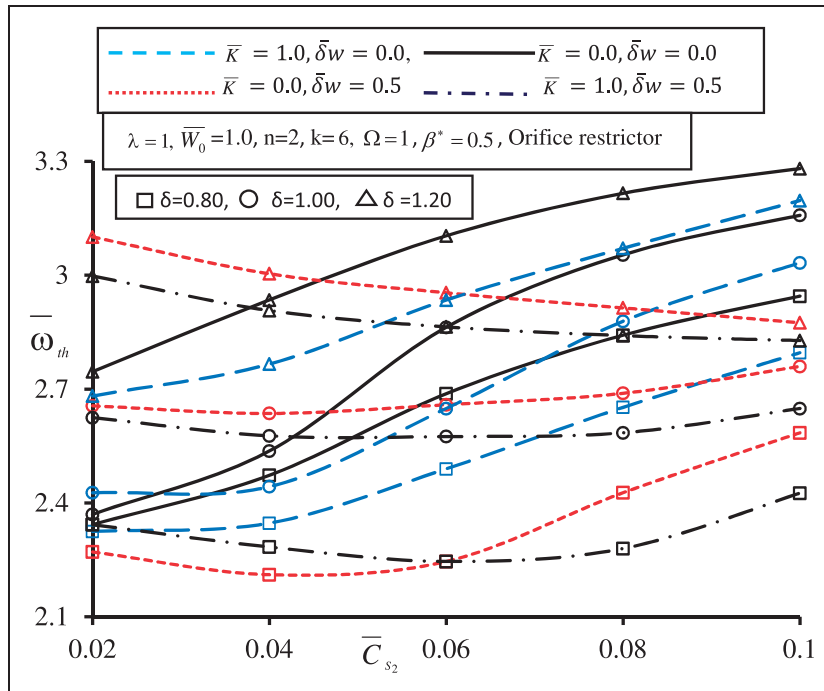


Figure 21. Threshold speed ($\bar{\omega}_{th}$) for asymmetric bearing configuration.

conditions. Figure 14 shows that the loss in the stiffness coefficients \bar{S}_{11} which occurs corresponding to $\bar{\delta}_w = 0.5$ may be compensated to some extent by selecting suitable values of \bar{C}_{S2} around 0.02 and 0.04 for an asymmetric hole-entry journal bearing configuration. Thus, it may be noted that a maximum value of stiffness coefficients can be achieved by a careful selection of the restrictor design parameter \bar{C}_{S2} at a particular value of the external load ($\bar{W}_0 = 1.0$).

Direct fluid-film damping coefficients (\bar{C}_{11} , \bar{C}_{22})

The results of fluid-film damping coefficient (\bar{C}_{11} , \bar{C}_{22}) for symmetric and an asymmetric two lobe hole entry worn hybrid journal bearing configurations have been presented in Figures 16 to 19. It can be observed from Figures 16 and 17 that the wear depth parameter ($\bar{\delta}_w$) has a predominant effect on \bar{C}_{11} and \bar{C}_{22} . As a consequence of this, considerable reduction in the value of $\bar{C}_{11}/\bar{C}_{22}$ is observed for both symmetric and asymmetric bearing configurations. Further, it is clear from Figures 16 to 19 that non-circular hybrid journal bearing with an offset factor ($\delta = 1.20$) have largest value of direct fluid-film damping coefficient (\bar{C}_{11} , \bar{C}_{22}) than circular hybrid journal bearing ($\delta = 1.0$) at the fixed value of $\bar{\delta}_w = 0.5$. It may also be noted that the value of $\bar{C}_{11}/\bar{C}_{22}$ decreases with an increase in the non-linearity factor (\bar{K}) of the lubricant and the wear depth parameter ($\bar{\delta}_w$). The value of the $\bar{C}_{11}/\bar{C}_{22}$ is minimum for the non-Newtonian lubricants ($\bar{\delta}_w = 0.5$, $\bar{K} = 1$). From Figures 16 to 19, it is clearly visible that the effect of non-Newtonian behavior of lubricants is to reduce the \bar{C}_{11} and \bar{C}_{22} . For a chosen value of external load $\bar{W}_0 = 1.0$ and wear depth

parameter $\bar{\delta}_w = 0.5$, the value of $\bar{C}_{11}/\bar{C}_{22}$ for an asymmetric configuration is less than that of a symmetric configuration. The maximum reduction of the order of 18.76% in the value of \bar{C}_{11} and of the order of around 18.34% in the value of \bar{C}_{22} are observed at $\bar{\delta}_w = 0.5$, $\bar{K} = 1$ and $\delta = 1.20$ for a symmetric bearing configuration than unworn circular hole entry journal bearing operating with Newtonian fluid. For an asymmetric bearing configuration, the maximum reduction in the value of $\bar{C}_{11}/\bar{C}_{22}$ of the order of 18.76% and 21.80% is observed at $\bar{\delta}_w = 0.5$, $\bar{K} = 1$, $\delta = 1.20$. Further, it is also noticed that the value of $\bar{C}_{11}/\bar{C}_{22}$ is largest for unworn hole entry journal bearing lubricated with Newtonian lubricant ($\bar{\delta}_w = 0.0$, $\bar{K} = 0$) for an offset factor greater than one ($\delta = 1.20$).

Stability threshold speed margin ($\bar{\omega}_{th}$)

Figures 20 and 21 indicate that the influence of wear depth parameter ($\bar{\delta}_w$) is to reduce the value of threshold speed margin ($\bar{\omega}_{th}$) for a specified value of an external load ($\bar{W}_0 = 1.0$). It is observed that the bearing with an offset factor greater than one ($\delta = 1.20$) have highest value of threshold speed margin ($\bar{\omega}_{th}$) than bearing with an offset factor ($\delta = 1.0, 0.80$) for the same chosen values of operating parameter. The noticeable observation from Figure 20 is that the value of $\bar{\omega}_{th}$ decreases with the increase in the value of wear depth parameter ($\bar{\delta}_w$). Further, it is observed that the non-linearity parameter (\bar{K}) has a marginal effect on the value of $\bar{\omega}_{th}$ of both bearing configurations. Figure 21 indicates that the stability threshold speed margin deteriorates increased in a value of wear depth parameter ($\bar{\delta}_w$) along with non-linear behavior

Table 3. Percentage change in performance characteristics of an orifice restrictor two lobe non recessed symmetric bearing configuration.^a

Offset factor (δ)	Percentage change									
	\bar{K}	$\bar{\delta}_w$	$\% \bar{h}_{\min}$	$\% \bar{Q}$	$\% \bar{P}_{\max}$	$\% \bar{S}_{11}$	$\% \bar{S}_{22}$	$\% \bar{C}_{11}$	$\% \bar{C}_{22}$	$\% \bar{\omega}_{th}$
0.80	0.0	0.0	2.16	7.91	1.54	-18.67	-17.08	-20.38	-13.19	-8.4
	1.0	0.0	-3.30	15.13	-12.34	-29.6	-24.57	-34.35	-28.94	-13.59
	0.0	0.5	-3.81	14.81	-3.30	-37.82	-29.74	-31.10	-33.52	-18.3
	1.0	0.5	-11.14	20.26	-15.62	-46.80	-37.85	-42.78	-45.83	-22.95
1.00	0.0	0.0								
	1.0	0.0	-4.5	8.94	-12.14	-9.83	-8.91	-17.93	-18.34	-4.4
	0.0	0.5	-12.96	10.39	16.64	-28.64	-17.87	-14.29	-24.10	-10.65
	1.0	0.5	-18.37	15.28	-1.64	-34.41	-26.84	-29.11	-38.20	-14.67
1.20	0.0	0.0	-13.39	-6.61	15.63	1.90	12.04	13.35	8.38	3.91
	1.0	0.0	-15.19	3.88	-1.07	0.1989	2.59	-5.53	-10.87	1.3
	0.0	0.5	-18.66	1.42	45.67	-40.06	-8.86	-5.46	-18.47	-9.54
	1.0	0.5	-23.48	10.77	17.65	-31.31	-18.20	-18.76	-32.64	-9.70

^a $\lambda = 1$, $\bar{W}_0 = 1.0$, $n = 2$, $k = 12$, $\Omega = 1$ and $\beta^* = 0.5$.

Table 4. Percentage change in performance characteristics of an orifice restrictor two lobe non recessed asymmetric journal bearing.^a

Offset factor (δ)	Percentage change									
	\bar{K}	$\bar{\delta}_w$	$\% \bar{h}_{\min}$	$\% \bar{Q}$	$\% \bar{P}_{\max}$	$\% \bar{S}_{11}$	$\% \bar{S}_{22}$	$\% \bar{C}_{11}$	$\% \bar{C}_{22}$	$\% \bar{\omega}_{th}$
0.80	0.0	0.0	0.92	3.96	13.46	-13.70	-10.72	-25.91	-16.19	-6.11
	1.0	0.0	-3.46	9.00	-3.79	-29.45	-22.12	-40.66	-33.68	-13.02
	0.0	0.5	-3.92	8.98	7.47	-48.84	-33.96	-37.55	-37.83	-21.55
	1.0	0.5	-13.70	11.36	1.30	-50.36	-35.12	-48.98	-50.47	-20.01
1.00	0.0	0.0								
	1.0	0.0	-4.29	6.25	-10.30	-15.38	-14.42	-22.70	-21.80	-7.4
	0.0	0.5	-15.06	3.34	39.24	-15.77	-16.00	-17.40	-27.15	-7.12
	1.0	0.5	-21.48	7.25	20.96	-21.56	-22.05	-34.51	-42.19	-10.0
1.20	0.0	0.0	-16.03	-4.20	26.96	17.48	15.65	-11.89	13.42	8.41
	1.0	0.0	-19.32	2.51	9.29	5.71	2.46	25.42	-11.89	2.51
	0.0	0.5	-23.59	-2.91	67.80	4.53	1.27	1.37	-19.30	3.71
	1.0	0.5	-28.25	2.86	40.90	2.56	-7.94	-20.71	-35.95	3.49

^a $\lambda = 1$, $\bar{W}_0 = 1.0$, $n = 2$, $k = 6$, $\Omega = 1$ and $\beta^* = 0.5$.

of the lubricant. Due to the combined influence of $\bar{\delta}_w = 0.5$ and $\bar{K} = 1.0$, the maximum reduction of 9.70% and 14.67% is observed in the value of $\bar{\omega}_{th}$ at $\delta = 1.20$ and $\delta = 1.0$ respectively, for a symmetric bearing configuration.

Further result presented in Figure 21 reveals that the loss of stability threshold speed margin can be compensated by selecting an appropriate value of restrictor design parameter $\bar{C}_{S_2} = 0.02$, $\bar{C}_{S_2} = 0.04$ at $\delta = 1.20$ for worn an asymmetric bearing configuration. It is observed from Figure 21 that the stability

of the journal bearing with offset factor $\delta = 1.20$, $\bar{K} = 0$ and $\bar{\delta}_w = 0$ have greater value of 8% threshold speed margin ($\bar{\omega}_{th}$) than circular hole entry bearing lubricated with Newtonian lubricant.

For a symmetric and an asymmetric bearing configuration, comparative performance characteristic parameters have been presented in Tables 3 and 4. The percentage change in the characteristics parameter is computed with respect to base bearing, i.e. unworn circular journal bearing lubricated with Newtonian lubricant. The comparative performance

Table 5. Dimensional values of performance characteristics for symmetric bearing configuration.

Performance characteristics of two lobe non recessed hybrid journal bearing										
(δ)	\bar{K}	$\bar{\delta}_w$	h_{\min} (mm)	$Q \times 10^4$ (mm ³ /s)	P_{\max} (N/mm ²)	S_{11} (MN/mm)	S_{22} (MN/mm)	C_{11} (MN-s/m)	C_{22} (MN-s/m)	ω_{th} rad/s
0.80	0.0	0.0	0.04420	3.5930	7.017	1.277	1.327	17.76	18.88	1531.2
	1.0	0.0	0.04184	3.8337	6.057	1.103	1.204	14.65	15.46	1446.6
	0.0	0.5	0.04162	3.8220	6.682	0.9763	1.124	15.37	14.46	1370.1
	1.0	0.5	0.03845	4.0045	5.831	0.8353	0.9946	12.77	11.78	1288.1
1.00	0.0	0.0	0.04327	3.3297	6.910	1.5702	1.600	22.32	21.76	1671.8
	1.0	0.0	0.04129	3.6277	6.065	1.4158	1.4577	18.31	17.76	1597.1
	0.0	0.5	0.03766	3.5955	8.061	1.1204	1.3145	19.13	16.49	1493.7
	1.0	0.5	0.03532	3.8386	6.797	1.0298	1.1708	15.82	13.44	1426.5
1.20	0.0	0.0	0.03747	3.1096	7.991	1.6001	1.7933	25.30	23.58	1694.4
	1.0	0.0	0.03636	3.4588	6.836	1.5733	1.6420	21.08	19.38	1737.2
	0.0	0.5	0.03520	3.3770	10.06	0.9410	1.4586	21.10	17.74	1512.2
	1.0	0.5	0.03311	3.6885	8.131	1.0785	1.3091	18.13	14.65	1509.6

presented in Tables 3 and 4 reveals that the combined influence of wear defect and non-linear behavior of the lubricant has significant effect on the bearing performance and must be considered in the analysis.

$$\% \left(\text{Performance characteristic} \right) = \left[\frac{\left(\text{Performance characteristic} \right)_{at \delta=0.80, 1.20, \bar{\delta}_w=0.0, 0.5 \bar{K}=0.0, 1.0} - \left(\text{Performance characteristic} \right)_{at \delta=1.0, \bar{\delta}_w=0.0, \bar{K}=0.0}}{\left(\text{Performance characteristic} \right)_{at \delta=1.0, \bar{\delta}_w=0.0, \bar{K}=0.0}} \right] \times 100$$

Numerical example

To illustrate practical use and present dimensional performance characteristics of a two lobe non recessed worn hybrid journal bearing system operated with non-Newtonian lubricant, a numerical example is presented here. The dimensional and operating parameters of the bearing presented in Table 1 are used to compute the dimensional values of static and dynamic performance characteristics. The dimensional values of static and dynamic performance characteristics of the two lobe non recessed journal bearing are presented in Tables 5 and 6 for symmetric and asymmetric journal bearing configuration, respectively.

Conclusion

The numerical study of two lobe non recessed worn hybrid journal bearing operating with non-Newtonian lubricant has been performed to find out the combined influence of wear and non-Newtonian lubricant on the performance characteristics of the non recessed hybrid journal bearing. On the basis of the numerically simulated results of this study, the following general conclusions are drawn as follows.

1. The combine influence of wear and non-linear behavior of lubricants is quite profound on the performance of a two lobe non recessed hybrid bearing system with different offset factor.
2. The fluid-film pressure distribution gets altered by the non-Newtonian behavior of the lubricant. For unworn bearing, maximum fluid-film pressure decreases with an increase in the value of non-linearity factor (\bar{K}) and for the same operating condition, worn journal bearing operates at higher value of fluid-film pressures.
3. The minimum fluid-film thickness (\bar{h}_{\min}) gets decreased as the lubricant behavior becomes more non-linear as compared to journal bearing operating with Newtonian lubricants. An increase in the value of wear depth parameter ($\bar{\delta}_w$), increases eccentricity of the bearing and journal tend to go into defect footprint, so the fluid-film thickness reduces for worn bearing. However, an increase in the value restrictor design parameter (\bar{C}_{S2}) recompensates this loss.
4. The fluid-film thickness (\bar{h}_{\min}) for worn symmetric non recessed journal bearing configuration ($\delta = 1.20$) is reduced by 23.48 percent vis-à-vis

Table 6. Dimensional values of performance characteristics for asymmetric bearing configuration.

Performance characteristics of two lobe non recessed hybrid journal bearing										
(δ)	\bar{K}	$\bar{\delta}_w$	h_{\min} (mm)	$Q \times 10^4$ (mm ³ /s)	P_{\max} (N/mm ²)	S_{11} (MN/mm)	S_{22} (MN/mm)	C_{11} (MN-s/m)	C_{22} (MN-s/m)	ω_{th} rad/s
0.80	0.0	0.0	0.04582	0.6735	4.717	0.5854	1.0004	19.63	20.37	1188.2
	1.0	0.0	0.04707	1.9403	4.358	0.4787	0.8745	15.72	16.12	1100.7
	0.0	0.5	0.04986	1.9400	4.868	0.3471	0.7416	16.54	15.11	992.8
	1.0	0.5	0.04208	1.9824	4.589	0.3368	0.7286	13.51	12.04	992.8
1.00	0.0	0.0	0.04876	1.7800	4.530	0.6786	1.1231	26.49	24.31	1265.6
	1.0	0.0	0.04667	1.8914	4.063	0.5742	0.9611	20.47	19.01	1171.0
	0.0	0.5	0.04143	1.8394	6.307	0.5716	0.9432	21.98	17.71	1175.4
	1.0	0.5	0.03829	1.9091	5.479	0.5323	0.8754	17.35	14.00	1138.3
1.20	0.0	0.0	0.04094	1.7051	5.749	0.7973	1.2989	33.23	27.57	1372.1
	1.0	0.0	0.03934	1.8247	4.951	0.7175	1.1507	25.34	21.42	1297.4
	0.0	0.5	0.03726	1.7281	7.601	0.7094	1.1374	26.86	19.62	1305.8
	1.0	0.5	0.03498	1.8309	6.383	0.6960	1.0338	21.00	15.57	1266.0

circular unworn hole entry journal bearing lubricated with non-Newtonian lubricant. For worn journal bearing lubricated with non-Newtonian and Newtonian lubricant, the subsequent fluid-film pattern has been observed.

$$\bar{h}_{\min}|_{\delta=1.20} < \bar{h}_{\min}|_{\delta=1.0} < \bar{h}_{\min}|_{\delta=0.80}$$

- The values of bearing fluid-film dynamic coefficients (\bar{S}_{11} , \bar{S}_{22} , \bar{C}_{11} , \bar{C}_{22}) get decreased for the damaged out bearing lubricated with non-Newtonian lubricants. Therefore, for a worn bearing system operated by non-Newtonian lubricant, the bearing designer will choose appropriate bearing geometry on the basis of following criteria to get improved values of fluid-film dynamic coefficients.

$$\bar{S}_{11/22}, \bar{C}_{11/22}|_{\delta=1.20} > \bar{S}_{11/22}, \bar{C}_{11/22}|_{\delta=1.0} > \bar{S}_{11/22}, \bar{C}_{11/22}|_{\delta=0.80}$$

- In general, the combined influence of wear depth parameter ($\bar{\delta}_w$) and non-linearity factor (\bar{K}) on the performance of two lobe non recessed journal bearing is to have a slight reduction in the value of stability threshold speed margin ($\bar{\omega}_{th}$).

Funding

This research received no specific grant from any funding agency in the public, commercial, or not-for-profit sectors.

Conflict of interest

None declared.

References

- Pinkus O. Analysis of elliptical bearing. *ASME Trans* 1956; 78: 965–973.
- Lund JW and Thomsen KK. A calculation method and data for the dynamic coefficient of oil lubricated journal bearing. In: *ASME design engineering conference*, Chicago, IL, ASME, 1978, 100118, pp.1–28.
- Flack RD and Lanes RF. Effects of three lobe bearing geometries on rigid rotor stability. *ASLE Trans* 1982; 25(2): 221–228.
- Garner DR, Lee CS and Martin FA. Stability of profile bore bearing: influence of bearing type selection. *Tribol Int* 1980; 13(5): 204–210.
- Li DF, Choy KC and Allaire PE. Stability and transient characteristics of four multilobe journal bearing configurations. *ASME J Lubr Tech* 1980; 102: 291–298.
- Goenka PK and Booker JF. Effect of surface ellipticity on dynamically loaded cylindrical bearing. *ASME J Lubr Tech* 1983; 105: 1–12.
- Singh A and Gupta BK. Stability analysis of orthogonally displaced bearings. *Wear* 1984; 97: 83–92.
- Rahmatabadi AD, Nekoeimehr M and Rashidi R. Micropolar lubricant effects on the performance of noncircular lobed bearings. *Tribol Int* 2010; 43(1–2): 404–413.
- Ghosh MK and Satish MR. Rotor dynamic characteristics of multi lobe hybrid bearings with short sills—part I. *Tribol Int* 2003; 36(8): 625–632.
- Ghosh MK and Satish MR. Rotor dynamic characteristics of multilobe hybrid bearings with short sills—part II. *Tribol Int* 2003; 36(8): 633–636.
- Bouyer J, Fillon M and Pierre-Danos I. Influence of wear on the behavior of a two-lobe hydrodynamic journal bearing subjected to numerous start ups and stops. *ASME J Tribol* 2007; 129: 205–208.
- Phalle Vikas M, Sharma Satish C and Jain SC. Influence of wear on the performance of a 2-lobe multirecess hybrid journal bearing system compensated with membrane restrictor. *Tribol Int* 2011; 44(4): 380–395.

13. Sharma Satish C, Phalle Vikas M and Jain SC. Performance of a noncircular 2-lobe multirecess hydrostatic journal bearing with wear. *Indus Lubr Tribol* 2012; 64(3): 171–181.
14. Rowe WB. Advances in hydrostatic and hybrid bearing technology. *Proc IMechE Part C: J Mechanical Engineering Science* 1989; 203(4): 225–242.
15. Awasthi RK, Sharma Satish C and Jain SC. Performance of worn non-recessed hole-entry hybrid journal bearings. *Tribol Int* 2007; 40(5): 717–734.
16. Soulas T and Andres LS. Performance of damaged hydrostatic bearings: predictions versus experiments. *ASME J Tribol* 2003; 125: 451–456.
17. Laurant F and Childs DW. Measurement of rotor dynamic coefficients of hybrid bearings with (a) a plugged orifice (b) a worn land surface. *J Eng Gas Turbines Power* 2002; 124: 363–368.
18. Hashimoto H, Wada S and Nojima K. Performance characteristics of worn journal bearings in both laminar and turbulent regime. *Part 1: steady state characteristics*. *STLE Tribol Trans* 1986; 29: 565–571.
19. Kumar and Mishra SS. Stability of rigid rotor in turbulent hydrodynamic worn journal bearings. *Wear* 1996; 193: 25–30.
20. Kumar and Mishra SS. Steady state analysis of non-circular worn journal bearings in non-laminar lubrication regimes. *Tribol Int* 1996; 29: 493–498.
21. Fillon M and Bouyer J. Thermo hydrodynamic analysis of a worn plain journal bearing. *Tribol Int* 2004; 37(2): 129–136.
22. Rajasekhar Nicodemus E and Sharma Satish C. Influence of wear on the performance of multirecess hydrostatic journal bearing operating with micropolar lubricant. *ASME J Tribol* 2010; 132(2): 021703–1–11.
23. Redcliff JM and Vohr JH. Hydrostatic bearings for cryogenic rocket engine turbopumps. *ASME J Lubr Tech* 1969; 91(3): 557–575.
24. Dufrane KF, Kannel JW and McCloskey TH. Wear of steam turbine journal bearings at low operating speeds. *J Lubr Tech* 1983; 105: 313–317.
25. Li XK, Gwynllyw DRh, Davies AR, et al. On the influence of lubricant properties on the dynamics of two-dimensional journal bearings. *J Non-Newtonian Fluid Mech* 2000; 93: 29–59.
26. Prashad H. The effects of viscosity and clearance on the performance of hydrodynamic journal bearings. *STLE Tribol Trans* 1988; 1(2): 113–123.
27. Wada S and Hayashi H. Hydrodynamic journal bearings by pseudo-plastic lubricants, part-i theoretical studies. *Bull JSME* 1971; 14(69): 268–278.
28. Tayal SP, Sinhasan R and Singh DV. Finite element analysis of elliptical bearings lubricated by a non-Newtonian fluid. *Wear* 1982; 80: 71–81.
29. Wu Z and Dareing Don W. Non-Newtonian effects of powder-lubricant slurries in hydrostatic and squeeze-film bearings. *STLE Tribol Trans* 1994; 37(4): 836–842.
30. Sinhasan R and Sah PL. Static and dynamic performance characteristics of an orifice compensated hydrostatic journal bearing with non-Newtonian lubricants. *Tribol Int* 1996; 29(6): 515–526.
31. Sharma SC, Jain SC and Sah PL. Effect of non-Newtonian behaviour of lubricant and bearing flexibility on the performance of slot-entry journal bearing. *Tribol Int* 2000; 33(7): 507–517.
32. Sharma SC, Jain SC and Sinhasan R. static and dynamic performance characteristics of orifice compensated hydrostatic flexible journal bearings with non-Newtonian lubricants. *STLE Tribol Trans* 2001; 44(2): 242–248.
33. Nagaraju T, Sharma SC and Jain SC. Influence of surface roughness on non-Newtonian thermo hydrostatic performance of a hole-entry hybrid journal bearing. *ASME J Tribol* 2007; 129(3): 595–602.
34. Dowson D. A generalized Reynolds equation for fluid film lubrication. *Int J Mech Eng Sci* 1962; 4(2): 159–170.
35. Rowe WB, Xu SX, Chong FS and Weston W. Hybrid journal bearings with particular reference to hole-entry configuration. *Tribol Int* 1982; 15(6): 339–348.
36. Scharrer JK, Hecht RF and Hibbs RI. The effects of wear on the rotordynamic coefficients of hydrostatic journal bearing. *ASME J Tribol* 1991; 113: 210–213.

Appendix

Notation

a_b	bearing land width, mm
$\bar{a}_b = a_b/L$	L and width ratio
c	radial clearance, mm
C_{ij}	damping coefficients ($i, j = 1, 2$), N.s.mm ⁻¹
$\bar{C}_{ij} = C_{ij}(c^3/\mu R_J^4)$	
$\bar{C}_{S2} = (\pi d_o^2 \mu \psi_d / 4c^3)(2/\rho p_s)^{1/2}$	restrictor design parameter
C_1	clearance due to circumscribed circle on the bearing, mm
C_2	clearance due to inscribed circle on the bearing, mm
d_o	orifice diameter, mm
D	journal diameter, mm
e	journal eccentricity, mm
E	Young's modulus of elasticity, N.mm ⁻²
F	fluid-film reaction ($\partial h/\partial t \neq 0$), N
$[\bar{F}]$	fluidity matrix
$(\bar{F}, \bar{F}_o) = (F, \bar{F}_o)/p_s R_J^2$	
F_o	fluid-film reaction ($\partial h/\partial t = 0$), N
F_x, F_z	components of fluid-film reactions in X and Z direction ($\partial h/\partial t \neq 0$), N
g	acceleration due to gravity, m.s ⁻²
h	nominal fluid-film thickness, mm
$(\bar{h}) = (h)/c$	
L	bearing length, mm
N_i, N_j	shape functions
O_j, O_{Li}	journal center, lobe center
$\{\bar{R}_H\}$	vector due to hydrodynamic terms

R_J, R_L, R_b	radius of journal, lobe and bearing, mm	$\varepsilon = e/c$	eccentricity ratio
$\{\bar{R}_{Xj}\}, \{\bar{R}_{Zj}\}$	right hand side vectors due to journal center velocities	$\lambda = L/D$	aspect ratio
p	pressure, N.mm ⁻²	μ	dynamic viscosity of lubricant, N.s.m ⁻²
$\{\bar{p}\}$	nodal pressure vector	ρ	density of the lubricant kg mm ⁻³
$\bar{p}, \bar{p}_c, \bar{p}_{\max} = (p, p_c, p_{\max})/p_s$		$\tau = t(c^2 p_s / \mu R_J^2)$	
p_s	lubricant supply pressure	ϕ	altitude angle
Q	bearing flow, mm ³ .s ⁻¹	ψ_d	coefficient of discharge for orifice
$\bar{Q} = Q(\mu/c^3 p_s)$		ω_I	(g/c) ^{1/2} , rad.s ⁻¹
$\{\bar{Q}\}$	nodal flow vector	ω_J	journal rotational speed, rad.s ⁻¹
S_{ij}	stiffness coefficients ($i, j = 1, 2$), N.mm ⁻¹	ω_{th}	threshold speed, rad.s ⁻¹
$\bar{S}_{ij} = S_{ij}(c/p_s R_J^2)$		$\delta = C_1/C_2$	offset factor
t	time, s	$\bar{\omega}_{th} = \omega_{th}/\omega_I$	
W_o	external load, N	$\Omega = \omega_J(\mu R_J^2/c^2 p_s)$	speed parameter
$\bar{W}_o = W_o/p_s R_J^2$		Subscripts and superscripts	
X, Y, Z	Cartesian coordinates	b	bearing
$\bar{X}_L^i, \bar{Z}_L^i = (X_L^i, Z_L^i)/c$		i	lobe number
X_J, Z_J	coordinates of steady state equilibrium journal center from geometric center of bearing, mm	J	journal
$(\bar{X}_J, \bar{Z}_J) = (X_J, Z_J)/c$		l	lobe
		max	maximum
		min	minimum
		R	restrictor
		s	supply
Greek symbols		Symbols	
$\alpha, \beta = (X, Y)/R_J$	circumferential and axial coordinates	\cdot	first derivative with respect to time
α_b, α_e	start and end of the worn region	$*$	concentric operation
$\beta^* = p^*/p_s$	concentric design pressure ratio	$-$	corresponding non-dimensional parameter
δ_w	wear depth, mm		
$\bar{\delta}_w = \delta_w/c$			